

General Disclaimer

One or more of the Following Statements may affect this Document

- This document has been reproduced from the best copy furnished by the organizational source. It is being released in the interest of making available as much information as possible.
- This document may contain data, which exceeds the sheet parameters. It was furnished in this condition by the organizational source and is the best copy available.
- This document may contain tone-on-tone or color graphs, charts and/or pictures, which have been reproduced in black and white.
- This document is paginated as submitted by the original source.
- Portions of this document are not fully legible due to the historical nature of some of the material. However, it is the best reproduction available from the original submission.



(NASA-CR-166711) ANTENNA PATTERN N82-11338
MODIFICATION FOR SINGLE REFLECTOR ANTENNAS
Final Report (Systems and Applied Sciences
Corp.) 51 p HC A04/MF A01 CSCI 20N Unclass
G3/32 01606



**SYSTEMS AND APPLIED
SCIENCES CORPORATION**
6811 KENILWORTH AVENUE
RIVERDALE, MARYLAND 20840

**ANTENNA PATTERN MODIFICATION FOR
SINGLE REFLECTOR ANTENNAS**

Final Report

January, 1981

Contract No. NAS5-25993

**ANTENNA PATTERN MODIFICATION FOR
SINGLE REFLECTOR ANTENNAS**

Final Report

Contract No. NAS5-25993

January, 1981

Prepared For:

**T.G. Cherrix
National Aeronautics and Space Administration
Goddard Space Flight Center
Greenbelt, Maryland 20771**

Prepared By:

**A.S. Milman
Systems and Applied Sciences Corporation
6811 Kenilworth Avenue
Riverdale, Maryland 20840**

TABLE OF CONTENTS

	PAGE
ABSTRACT	1
INTRODUCTION	3
I. MATHEMATICAL MODEL	7
II. THE ANTENNA PATTERN	12
III. NUMERICAL STUDY	13
IV. FOURIER TRANSFORMS AND THE RELATIONSHIP TO A LINEAR FILTER	18
V. CONCLUSIONS	32
ACKNOWLEDGEMENT	34
REFERENCES	35
TABLE CAPTIONS	36
TABLE 1.	37
TABLE 2.	38
TABLE 3.	39
TABLE 4.	40
TABLE 5.	41
TABLE 6.	42
TABLE 7.	43
FIGURE CAPTIONS	44
FIGURES 1a. - 1j.	45
FIGURE 2.	46
FIGURE 3.	47

ABSTRACT

This paper describes a method for correcting antenna temperatures observed with a single-reflector antenna for the effects of side lobes. The contribution from side lobes is a severe problem for earth-viewing microwave antennas, since the contrast in brightness between land and ocean is very high. The method developed here for correcting for the antenna side lobes estimates each brightness temperature as a linear combination of the antenna temperatures; therefore, it is suitable for conditions where the data rates are very high.

Any linear combination of the observed antenna temperatures is equivalent to the antenna temperature that would have been observed by an aperture with some other antenna pattern, which we call the "effective" power pattern. It is shown that this effective power pattern can be chosen so that it has lower sidelobe levels than the original power pattern.

Another problem is to match the areas observed at two frequencies (where the beam patterns will be different) so that meaningful comparisons can be made. This can be done using a simple extension of the material reported here.

A simple (Gaussian) beam pattern is chosen as an example; some representative results show that it is possible to suppress the side lobes at the expense of only minimal noise amplification and broadening of the main beam. It is also possible to smooth the observations

so that the noise is reduced, the side lobe level reduced,
and the main beam broadened only by about 10%.

INTRODUCTION

This paper describes a method for processing the data from a scanning microwave radiometer so as to modify the antenna pattern of the instrument. This method can be employed for correcting the data from mechanically-scanned microwave instruments that view the earth from space. Two such instruments—the Scanning Multichannel Microwave Radiometer on NIMBUS-7 and SEASAT-1 and the Large Antenna Multichannel Microwave Radiometer under study for the NOSS satellite—use a single antenna to make observations simultaneously at frequencies from 6.6 to 37 GHz. These antennas are conically scanned; i.e., the antenna points away from the nadir axis and is rotated about the nadir axis. The result is that the boresight traces a cone whose axis is in the nadir direction. The angle of incidence of the boresight on the earth's surface is constant. The two problems to be addressed in the data processing are: i) to modify the antenna pattern at the lowest frequency to reduce the level of the side lobes, and ii) to smooth the higher-frequency observations so that they can be compared with the lowest-frequency observation.

Many authors have studied the resolution limits imposed by an aperture of finite size (e.g., Schell 1969, and Buck and Gustincic 1967). Methods have been devised for correcting for side lobes in interferometer measurements (Högbom 1974) or for single-reflector antennas (e.g., Chow and Pelletier 1974, Emerson et al. 1979, and Njoku 1980). All of these methods require extensive data processing; the data rates from satellite instruments are high enough to preclude the use of these methods.

Also, attention seems to have been focused on trying to improve the resolution in the main beam (e. g., Classen and Fung 1974 and Stogryn 1978); it is shown in a later section that this must be accompanied by amplification of the noise in the observations. The focus of this paper is to consider ways to decrease the level of the side lobes of the antenna without amplifying the noise greatly. In general, little can be effectively done to improve the main-lobe resolution (because of noise amplification), but the effects of the side lobes can be suppressed.

The method presented here is to find a set of coefficients M_i so that the estimated brightness temperature at a point is given by

$$\hat{B}_j = \sum M_i T_i$$

where T_i is the antenna temperature observed at the point (x_i, y_i) .

Let $P(x, y)$ be the true power pattern of the antenna, and $Q(x, y)$ be a desired power pattern. The aim is to find a set of coefficients M_i so that the estimated brightness temperature \hat{B}_j is the same as the antenna temperature that would have been observed with an antenna that had the power pattern $Q(x, y)$. It will turn out that $Q(x, y)$ cannot be chosen arbitrarily—e.g., it is not possible to use a delta function—and that any increase in the spatial resolution will be accompanied by an increase in the noise in the estimated value \hat{B} . In this paper, emphasis will be placed on finding patterns $Q(x, y)$ that have low side-lobe levels. Suppression of the far sidelobe response is important for earth-viewing satellites, since at microwave frequencies the contrast in brightness temperature between land and ocean is on the order of 100 K; observations of the ocean will be useless when a few percent of the power comes from land areas.

Section I will discuss the mathematical methods employed to correct the antenna pattern using a matrix technique. A particular antenna power pattern is chosen for study and described in Section II; some numerical results are given in Section III. In particular, estimates are found for the error in the estimated brightness temperature and the factor by which the instrument

noise is amplified in the data processing. The problem of unwanted noise amplification is a common one in remote sensing problems—e.g., see Foster (1961) and Fleming (1976) for a review of related problems. Methods that do not treat the noise amplification problem from the beginning—such as the one proposed by Njoku (1980)—usually run into serious difficulties.

In Section IV, the problem will be looked at by treating the antenna as a spatial filter (this is, in part, an extension of the discussion given by Schell (1969); it also addresses a significantly different problem). This analysis is included to illustrate the properties and limitations of antenna pattern modification; it does not produce a workable method for performing the required calculations.

The problem of correcting the antenna patterns is thus addressed from two viewpoints. One is that of matrix operations, where the elements of the matrices are integrals of the antenna pattern: this formulation is directly applicable to developing algorithms. The other viewpoint is that of analysis of the problem by treating the antenna as a spatial filter, and using Fourier transforms of the antenna pattern: this approach leads to an understanding of the problem, but is not suitable for performing calculations.

I. MATHEMATICAL MODEL

a) The matrix formulation

In this section the matrix formulae used to perform the antenna pattern modifications are derived. Let $P(x,y)$ be the true antenna pattern at the lowest frequency used for observations; the problem is to find a set of coefficients that transform $P(x,y)$ into some more suitable effective pattern. We suppose that the antenna is pointing toward a plane far from the antenna; the plane is normal to the boresight of the antenna and the antenna is moved to various points (x_i, y_i) .

When the antenna is pointing at (x_i, y_i) , the antenna temperature is given by

$$T_i = \int_{-\infty}^{\infty} \int_{-\infty}^{\infty} P_i(x,y) B(x,y) dx dy \quad (1)$$

where $B(x,y)$ is the brightness distribution and

$$P_i(x,y) = P(x_i - x, y_i - y). \quad (2)$$

The estimated brightness temperature \hat{B}_j at the point (x_j, y_j) will be given by

$$\hat{B}_j = \sum_i M_i T_i \quad (3)$$

where, in fact, the coefficients M_i may depend on the position (x_j, y_j) . Let $Q(x, y)$ be the desired effective antenna pattern. Since

$$\hat{B} = \int_{-\infty}^{\infty} \int_{-\infty}^{\infty} \sum_i M_i P_i(x, y) B(x, y) dx dy \quad (4)$$

we want

$$Q(x, y) = \sum_i M_i P_i(x, y). \quad (5)$$

The coefficients M_i can be found from a least-squares fit of $P(x, y)$ to $Q(x, y)$.

The error in the fit will be

$$\chi^2 = s^2 \int_{-\infty}^{\infty} \int_{-\infty}^{\infty} \left[Q(x, y) - \sum_i M_i P_i(x, y) \right]^2 dx dy + \sigma^2 \sum_i M_i^2 \quad (6)$$

where σ^2 is the noise in the radiometer, s^2 the variance of $B(x, y)$.

Note that χ^2 consists of two terms; one is due to the difference between $Q(x,y)$ and the fitted value. The error introduced by that term is proportional to the variance in the brightness distribution s^2 . The other term is due to amplification of the noise in the measured antenna temperatures. The constants M_i are found from differentiating equation 6 with respect to each M_i and equating the result to zero. The resulting effective antenna pattern is given by

$$\Psi(x,y) = \sum M_i P_i(x,y). \quad (7)$$

The difference between equations 5 and 7 is that $Q(x,y)$ is what is desired as the effective power pattern; $\Psi(x,y)$ is what can be achieved.

Define

$$R_i = \int_{-\infty}^{\infty} \int_{-\infty}^{\infty} P_i(x,y) Q(x,y) dx dy \quad (8)$$

and

$$P_{ij} = \int_{-\infty}^{\infty} \int_{-\infty}^{\infty} P_i(x,y) P_j(x,y) dx dy. \quad (9)$$

Then the values of M_i that minimize χ^2 are given by

$$\underline{M} = \left[\underline{P} + (\sigma^2/s^2) \underline{I} \right]^{-1} \underline{R} \quad (10)$$

where the elements of \underline{P} are P_{ij} . The matrix \underline{P} is positive definite, so none of the eigenvalues of $(\underline{P} + (\sigma^2/s^2) \underline{I})$ is

less than or equal to zero. The matrix is non-singular and its inverse exists. This solution is similar to one given by Foster (1961). The effect of using equation 10 is to balance the closeness of the fit of Ψ to Q against letting the noise amplification become too large.

b) Pattern-matching at higher frequencies

The method for matching the effective patterns at higher frequencies is a simple extension of what has been done so far. Since the beam is broadest at the lowest frequency, the effective pattern $\Psi_0(x,y)$ must be found first for the lowest frequency. Then, letting $\Psi_1(x,y)$ be the effective pattern at a higher frequency, the requirement that $\Psi_0 = \Psi_1$ is equivalent to finding a different set of coefficients M_i' that satisfy

$$\Psi_0(x,y) = \Psi_1(x,y) = \sum M_i' P_1(x-x_i, y-y_i) \quad (12)$$

where $P_1(x,y)$ is the antenna pattern at the higher frequency. A solution to equation 12 always exists with $\sum M_i'^2 < 1$ that corresponds to a smoothing of the antenna temperatures at the higher frequency.

II. THE ANTENNA PATTERN

This section describes the antenna pattern used to illustrate the method described in the previous section. This pattern was chosen so that the computations can be handled analytically.

The antenna gain pattern is given by

$$P(\theta) = 0.1475 e^{-\theta^2/2} + 0.0067 e^{-\theta^2/10} \quad (1)$$

where $\theta^2 = x^2 + y^2$. $P(\theta)$ is normalized so that its integral over all space is equal to one. The approximate half-power beamwidth (FWHM) is $2\sqrt{2\ln 2}$. If the main beam is defined to be 2.5 times the FWHM, then the main-beam efficiency is 90%.

This pattern has significant contributions from the side lobes (cf Figure 1-a); in the next section results are given for attempts to reduce those side lobes.

III. NUMERICAL STUDY

Examples are given in this section of how the real power pattern of an antenna can be modified to suppress the side lobes. Some care must be taken in choosing the form for $Q(x,y)$, the desired pattern. After some trial calculations, it became apparent that fitting to a boxcar function (e. g., equation IV-1) gives poor results; the main beam is fattened and the sidelobe levels are increased. A reasonable form for $Q(x,y)$ is a Gaussian

$$Q(x,y) = \frac{1}{2\pi a^2} e^{-\theta^2/2a^2} \quad (1)$$

where $\theta^2 = x^2 + y^2$. Then

$$R_i = \frac{0.1475}{a^2 + 1} \exp\{-\theta_i^2/(2a^2+2)\} + \frac{0.0067}{.2a^2+1} \exp\{-\theta_i^2/(2a^2+10)\} \quad (2)$$

where $\theta_i^2 = x_i^2 + y_i^2$. Then the coefficients P_{ij} are given by

$$P_{ij} = 0.0494 \left[\exp(-\theta_{ij}^2/4) + 0.179 \exp(-\theta_{ij}^2/12) \right. \\ \left. + 0.0144 \exp(-\theta_{ij}^2/20) \right] \quad (3)$$

where $\theta_{ij}^2 = (x_i - x_j)^2 + (y_i - y_j)^2$.

If $\sum M_i P_i(x,y)$ is going to represent an effective antenna pattern, it is necessary that $\sum M_i = 1$. However, there is a unique solution to equation I-9; in general, the coefficients M_i will not quite be normalized. Therefore define $c = \sum M_i$; $M_i' = M_i/c$ is a normalized set of coefficients. This is the solution to the equation

$$(\underline{P} + \eta^2 \underline{I}) \underline{M} = c \underline{R} \quad (5)$$

which arises if we let $Q'(x,y) = c Q(x,y)$; $\eta^2 = \sigma^2/s^2$. The error in the fit—equation I-6—can be written

$$\chi^2 = \sum M_i M_j P_{ij} - 2c \sum M_i R_j + c^2 K + \eta^2 \sum M_i^2. \quad (6)$$

Multiplying equation I-9 by \underline{M}^t and substituting into equation 7,

$$\chi^2 = s^2 (c^2 K - c \underline{M} \cdot \underline{R}) \quad (7)$$

where $K = \int_{-\infty}^{\infty} \int_{-\infty}^{\infty} Q(x,y)^2 dx dy$.

Experience has shown that, if $Q(x,y)$ is suitably chosen, c differs from unity by only a few percent.

One important parameter in the modelling of the antenna pattern correction is the spacing of the observations of antenna temperature Δx . Once the orbital altitude (and therefore the satellite velocity) and the scan rate have been chosen, the time spent observing a region is proportional to its area; therefore the noise in T_i is proportional to $(\Delta x)^{-2}$. This effect has been included implicitly in the calculations reported here; the

quoted signal-to-noise ratio η^{-2} is divided by $(\Delta x)^2$ —i.e., the signal-to-noise ratio is always given as the ratio of the variance in brightness to the noise for an integration time corresponding to $\Delta x = 1$.

b) Results

The problem now is to choose values of Δx , the interval at which the antenna temperatures are sampled, a^2 , the width of the function $Q(x,y)$, and the signal-to-noise ratio η^{-2} , which is treated as a free parameter. We have performed calculations with a variety of different values of these parameters; some combinations give good results, and others do not. It is not possible to quantify each resulting antenna pattern with only a few numbers; some representative patterns are shown in Figure 1, and more are described in Tables 1 and 2. Since the purpose of modifying the antenna pattern is to reduce the level of the far sidelobes, these tables list the values of x for which the power is reduced by 10 db and by 20 db. Where there is a sidelobe level is higher than -20 db, the point where the main lobe is -20 db from the peak, and also the point where the side lobe is -20 db from the peak are both given. The levels of the side lobes are given in the last column. The first column of the tables lists the value of a^2 , the second the signal-to-noise ratio used (η^{-2}), and the third the resulting noise amplification factor α^2 .

Figure 1 shows the patterns when $\Delta x = 1$ (i. e., the antenna temperatures are sampled every half-beamwidth), $a^2 = 1$, and $\eta^{-2} = 10, 10^2, 10^3$, and ∞ . Figure 1-a shows the original antenna pattern and the pattern for a Gaussian of width 1. In some ways, the most interesting pattern is shown in Figure 1-b, where $\eta^{-2} = 10$; the noise amplification factor is 0.079. That is, this pattern represents a considerable

smoothing of the raw data, but the effective antenna pattern is not stronger at $x > 4.2$ than the original pattern. This pattern has, instead, the property that the noise is reduced, and only the main beam is fattened. Figures 1-c to 1-e show what happens as the signal-to-noise ratio is increased: the main beam gets narrower, the noise amplification increases, and the sidelobes (which are alternately negative and positive) appear. Figure 1-e shows that a Gaussian beam with width 1 can be achieved with a noise amplification of only 1.58.

Figure 1-f is included to show that it is not possible to narrow the antenna pattern beyond certain limits. This is an attempt to fit the antenna pattern to a Gaussian with $a^2 = \frac{1}{2}$; $\eta^{-2} = \infty$. Even though the noise amplification factor is 235, the fit is not all that good: there are three sidelobes at about -20 db or higher.

Figure 1-g is included to show how the spacing of the observed antenna temperatures Δx influences the the width of the effective antenna pattern. The curves in Figures 1-c and 1-g both have $S/N = 100$ and $a^2 = 1$; the sampling interval in Figure 1-g is twice that of Figure 1-c. The former pattern is not an improvement over the original pattern at all; the side lobes are higher and the main beam wider. In general, it seems from the computations we have done that the minimum sampling interval will be about one half of the half-power beamwidth (the maximum sampling interval size will be discussed in the next section).

The quality of the corrected pattern can be measured by two additional numbers. The resolution is measured by the full width at half-maximum (FWHM) of the beam. A measure of how well the side lobes are suppressed is given by x_{1000} . Let the brightness distribution be given by $B = 1$ for $x < x_b$, and $B = 0$ for $x > x_b$. Then the antenna temperature is a function of x_b ; x_{1000} is the value of x_b where the antenna temperature $< 10^{-3}$. For the original beam, the FWHM is 2.4, and $x_{1000} = 5.9$. Tables 3 and 4 list the values for the corrected antenna patterns.

From Table 3, we can see that, for $a^2 = 1$, $S/N = 1000$, and $\Delta x = 1$, the FWHM is 2.6 (10% larger than the original beam), but $x_{1000} = 2$. The noise amplification is 0.5. Therefore, for this combination of parameters, the distance at which the contribution from the side lobes $= 10^{-3}$ is reduced from 5.9 to 2.0; the main beam is broadened only by 10%, and the noise is reduced by a factor of 2. This is certainly an improvement over the original beam.

IV. FOURIER TRANSFORMS AND THE RELATIONSHIP TO A LINEAR FILTER

So far, the discussion of the antenna pattern correction problem has been in terms of integrals of the power pattern and matrix operations. The following discussion will be in terms of the Fourier transform of the effective power pattern and the aperture illumination distribution. The discussion is limited in two respects that make it inapplicable to the specific problem of correction the data from a mechanically scanned radiometer looking at the earth, but the discussion will aid in the understanding of the processes. The restrictions are 1) the antenna temperatures are observed at regularly-spaced intervals Δ , and 2) the power pattern does not change as function of position (for a conically-scanning antenna, the power pattern rotates as the antenna scans).

In the previous discussion, the function $Q(x,y)$ was introduced as the "desired" antenna pattern; there was, however, no indication as to what a desirable form might be for $Q(x,y)$.

In this section, the Fourier transform of $Q(x,y)$ will be seen to be a smoothing function that broadens $\Psi(x,y)$ (the effective power pattern); it turns out that this smoothing is what makes it possible to reduce the level of the sidelobes.

a) Relation to aperture illumination distribution

To start off, let $P(x,y)$ be the power pattern, and $\bar{P}(x,y) = P(-x,-y)$. Let $Q(x,y)$ and $P(x,y)$ have Fourier transforms $q(s,t)$ and $p(s,t)$; the Fourier transform of $\bar{P}(x,y)$ is $\bar{p}(s,t)$. (Note that $\bar{p}(s,t)$ is the complex conjugate of $p(s,t)$).

The antenna temperatures are sampled at an interval Δ ;
define the function

$$\begin{aligned} \Pi(x) &= 1 & |x| < \frac{1}{2} \\ \Pi(x) &= 0 & |x| > \frac{1}{2}. \end{aligned} \quad (1)$$

The coefficients P_{ij} were defined in equation I-8;

P_{ij} is the convolution $P(x,y) * \bar{P}(x,y)$ evaluated at $(x_j - x_i, y_j - y_i)$ (where $f * g$ denotes the convolution of f with g).

The Fourier transform of $P * \bar{P}$ is $p(s,t) \bar{p}(s,t)$. The coefficients R_i defined in equation I-7 are values of $Q(x,y) * P(x,y)$ and the Fourier transform is $q(s,t) \bar{p}(s,t)$. If the expression for χ^2 (equation I-6) is differentiated with respect to M_j and the result set equal to zero, the resulting equations can be written

$$\begin{aligned} \int_{-\infty}^{\infty} \int_{-\infty}^{\infty} \left[p(s,t) \bar{p}(s,t) \right] M_j e^{2\pi i \{ (x_i - x_j) s + (y_i - y_j) t \}} \\ - \bar{p}(s,t) q(s,t) e^{2\pi i (x_i s + y_i t)} \Big] ds dt + \eta^2 M_i = 0. \end{aligned} \quad (2)$$

Now introduce the function

$$m(s,t) = \sum M_j e^{-2\pi i (x_j s + y_j t)}; \quad (3)$$

this finite Fourier transform has the inverse

$$\int_{-\infty}^{\infty} \int_{-\infty}^{\infty} \Pi(s/\Delta) \Pi(t/\Delta) e^{2\pi i (x_i s + y_i t)} m(s,t) ds dt \quad (4)$$

where Δ is the sampling interval.

Putting equation 3 into equation 2, and using equation 4 to include the M_j term,

$$m(s,t) = \frac{\bar{p}(s,t)q(s,t)}{p(s,t)\bar{p}(s,t) + \eta^2\Pi(s/\Delta)\Pi(t/\Delta)} \quad (5)$$

The effective power pattern, given by $\Psi(x,y) = \sum M_j P_j(x,y)$, is the Fourier transform of

$$\psi(s,t) = \frac{p(s,t)\bar{p}(s,t)q(s,t)}{p(s,t)\bar{p}(s,t) + \eta^2\Pi(s/\Delta)\Pi(t/\Delta)} \quad (6)$$

In the case $Q(x,y) = \delta(x)\delta(y)$, so that $q(s,t) = 1$, this solution is that of, for example, Schell (1969, p 573). If the antenna is viewed as a spatial filter, this case becomes what Davenport and Root (1958) call an "optimum linear filter." Equation 6 is a generalization of a Wiener filter (Wiener 1960). The role of $Q(x,y)$ is now clearly seen: $Q(x,y)$ is convolved with the Wiener filter and broadens it.

The question that has been postponed until now is, What is the meaning of \hat{B} , the estimated brightness temperature? What is meant by the notion of the true brightness distribution must now be examined.

One notion of the true brightness temperature $B(x,y)$ might be that of the brightness temperature at the point (x,y) . This definition will not do, however, since this can only be observed with an antenna with an infinite aperture. Another notion is that the true value of $B(x,y)$ is given by a uniformly weighted average over a finite area. This is equivalent to choosing $Q(x,y) = 1$ within that area,

and = 0 outside the area. The aperture illumination function $p(s,t)$ goes to zero at the edges of the aperture; therefore the behavior of $q(s,t)$ at large spatial frequencies cannot affect $\psi(s,t)$ and are lost in $\Psi(x,y)$. Therefore the notion of the true value of $B(x,y)$ being a uniformly weighted average over a finite area Δ is also not useful.

The only useful definition of the true value of $B(x,y)$ is a non-uniformly weighted average over an infinite area (where the weights become vanishingly small suitably far from the direction the antenna is pointing); the weight is given exactly by $\Psi(x,y)$. The point here is that only the last notion of the true brightness distribution is observable with a finite-aperture antenna; therefore the quality of the modified antenna pattern $\Psi(x,y)$ must be measured against some realizable pattern. For example, if the error is measured as being the difference between $\Psi(x,y)$ and a delta-function, the best fit will be found to be one with a narrow main lobe, and high side lobes that alternate sign. This may be a good solution mathematically, but is very far from being a useful correction to the data.

b) Noise amplification

The noise amplification is found from

$$\alpha^2 = \int_{-\infty}^{\infty} \int_{-\infty}^{\infty} \{m(s,t)\}^2 ds dt. \quad (7)$$

The noise amplification will be large whenever $\psi(s,t)/p(s,t)$ is large; this places one constraint on what patterns can be synthesized. One immediate consequence is that any pattern $\Psi(x,y)$ that has non-zero spatial components where $p(s,t) = 0$ (i.e., $\psi(s,t)/p(s,t) \rightarrow \infty$) will also have infinite noise amplification. The relative magnitudes of the spatial components of $P(x,y)$ can be modified wherever those components are non-zero. A response cannot be created in those spatial components of $\Psi(x,y)$ that are zero in $P(x,y)$.

The noise amplification can be calculated for the case where the aperture is uniformly illuminated— $p(s) = (1 - |s|)\Pi(\frac{1}{2}s)$ —and the Wiener filter form for $\psi(s)$ is used:

$$m(s) = \frac{1 - |s|}{1 - |s| + \eta^2} \Pi(\frac{1}{2}s) \quad (8)$$

Then

$$\alpha^2 = \frac{1}{\eta} \tan^{-1}(1/\eta) - \frac{1}{1 + \eta^2} \quad (9)$$

(All of the examples given are for a one-dimensional aperture; a second dimension adds considerable complication but no new understanding.) If the Wiener filter is used, which is equivalent to choosing $Q(x)$ to be a δ -function, the noise amplification can become large—in fact, $\alpha^2 \rightarrow \infty$ as $\eta^2 \rightarrow 0$, although $\alpha^2 \eta^2$ remains finite—and it is partly to reduce the noise amplification that other forms for $Q(x)$ are sought.

c) A set of realizable patterns

The Fourier transform relations expressed above can be used to investigate the properties of realizable effective antenna patterns. We shall develop a complete set of possible antenna patterns—complete in the sense that any realizable pattern is a linear combination of these basis patterns—; for simplicity, only one-dimensional apertures are considered. The aperture has a width of one; the autocorrelation function of the electric field distribution in the aperture— $p(s)$ —will be zero outside the interval $(-1,1)$. Let $\Psi(x)$ be the effective antenna pattern and $\psi(s)$ its Fourier transform.

To start with, we must realize that it is possible to write $q(s)$ as

$$q'(s) = \frac{q(s) (p(s)^2 + \eta^2)}{p(s)^2} \quad (10)$$

for some $q(s)$; then $\psi(s) = q(s)$ and $m(s) = \psi(s) / p(s) = q(s) / p(s)$. The question then is, What are the possible forms that $q(s)$ might have?

The first requirement is that $m(s)$ must not be too large, since the noise amplification is $\int m(s)^2 ds$. The second requirement is that it be possible to write

$$m(s) = a_0 + \sum a_n \cos(n\pi\Delta s) \quad (11)$$

where $\Delta/2$ is the sampling interval; this requirement comes about from the definition of $m(s)$. In equation (11), attention is limited to symmetric antenna patterns, so the sine terms do not appear.

Consider, as an example, the case where $\Delta = 1$ and

the aperture is uniformly illuminated, so that $p(s) = 1 - |s|$. Then for $m(s)$ given in equation 11, the only aperture distributions that can be generated are linear combinations of

$$\psi_n(s) \cong (1 - |s|) \cdot \cos(n\pi s) \Pi(s/2). \quad (12)$$

The resultant antenna patterns are the Fourier transforms of $\psi_n(s)$, and are given by

$$\Psi_n(x) = \frac{2}{\pi^2} \frac{n^2 + 4x^2}{(n^2 - 4x^2)^2} \{1 - (-1)^n \cos 2\pi x\}; \quad (13)$$

$\Psi_0(x) = \text{sinc}(x)$, which is the power pattern of a uniformly illuminated aperture. The functions Ψ_n are shown in Figure 2 for $n=0$ to 5. They have the property that they have maxima at $x = n/2$, and have zeroes at integral values of x (n even) or half-integral values of x (n odd). Individually, the $\Psi_n(x)$ are not useful antenna patterns; the aim is to find a linear combination that is useful (i. e., goes to zero quickly for $x > 1$).

For $Q(s)$ we now have to choose a desirable function, but it must be bandwidth limited. Several families of functions are possible; the one that we shall use as an example is

$$F_n(x) = 2^{n+1} n! \frac{j_n(2\pi x)}{(2\pi x)^n} \quad (14)$$

where $j_n(x)$ is the n^{th} spherical Bessel function of the first kind. The Fourier transform of $F_n(x)$ is $(1 - s^2)^n \Pi(s/2)$. Some other possible families are given in Table 5. The first five functions $F_n(x)$ are shown in Figure 3.

The noise amplification for each pattern $F_n(x)$ ($n > 0$) is

$$\alpha_n^2 = \frac{2}{2n-1} + \frac{n}{2n-1} \frac{2^{4n} \{(2n-1)!\}^2}{(4n-1)!}$$

$$= \int_{-1}^1 \frac{(1-s)^{2n}}{(1-|s|)^2} ds. \quad (15)$$

For $n = 0$, the noise amplification is infinite unless $\psi(s) = \Pi(s/2b)$ for some $b < 1$. Then $\alpha_0^2 = 2b/(1-b)$. The interesting feature of this family of functions is that α_n^2 is a decreasing function of n , and also the sidelobes (defined as anywhere $|x| > 1$) decrease with increasing n , although the width of the main lobe increases with increasing values of n .

In order that $F_n(x)$ be realizable, it must be possible to expand $(1-s^2)^n/(1-|s|)$ in a Fourier cosine series; i. e.,

$$\frac{(1-s^2)^n}{(1-|s|)} = a_0 + \sum_{n=1}^N a_n \cos(n\pi s). \quad (16)$$

When $m(s)$ is specified by such a series, the noise amplification can be found by

$$\alpha^2 = 2a_0^2 + \sum a_n^2. \quad (17)$$

The Fourier cosine series expansion coefficients for F_1 , F_2 , and F_3 are given in Table 6. Most of the noise amplification is due to the first term in each series.

Since, in practice, only a finite number of antenna temperatures can be included in the calculation, the series will have to be truncated after a few terms; this will not significantly reduce the noise amplification, but will change the shape

of the pattern. Table 6 shows that the relative importance of the higher-order terms increases as n increases; the price one pays for the low noise and low sidelobe level of the higher-order functions $F_n(x)$ is that more and more antenna temperatures must be included in the calculation of B , and the width of the main beam increases.

In the earlier section dealing with the matrix formulation of the problem, $Q(x,y)$ was chosen—somewhat arbitrarily—to be a Gaussian. The main reasons for this choice were that a Gaussian form leads to workable formulae, and that it fits the author's idea of what is a "desirable" antenna pattern. The role of $Q(x,y)$ is really to supply a goal toward which the antenna pattern is modified. When the formalism is changed to consider Fourier transforms, the use of a Gaussian becomes awkward, since the Fourier transform of a truncated Gaussian is not readily evaluated. For this reason—mathematical convenience—a different form was taken for Q ; i.e., $Q = F_n(x)$. Since the calculations discussed here are only for the purpose of elucidation of a method—a method that will not be practical in any event for real scanning antennas—the exact form of Q is not important. What is important is the realization that the antenna pattern can be modified by forming linear combinations of the antenna temperatures, and that the limitations as to what is possible—the aperture distributions ψ must be linear combinations of the functions $\psi_n(s)$ defined in equation 12—can be clearly stated.

Another feature that warrents comment is that explicit mention of the signal-to-noise ratio η^{-2} disappeared after equation 8 to be replaced with discussion of the noise amplification

α^2 . This emphasises somewhat better the idea that, in general, that the modification of the antenna pattern is performed only with a concomitant change in the level of the noise. One must be careful not to adopt a method of antenna pattern modification that produces a beautiful pattern but has infinite noise amplification.

d) Relationship between resolution and noise amplification

The functions $F_n(x) = 2^{n+1} (2\pi x)^{-n} j_n(2\pi x)$ increase in halfwidth as n increases; the full-widths at half-maximum (FWHM) are given in Table 7 for the first seven functions $F_n(x)$. It is not hard to show that, when the antenna pattern is modified, if the resolution is to increase, the noise amplification must increase also.

Define the fraction of the power contained in the interval $(-x_0, x_0)$ in the main beam, where $x_0 < \frac{1}{2}$, to be

$$\mu = \int_{-x_0}^{x_0} \psi(x) dx = 2 \int_0^1 \psi(s) \frac{\sin 2\pi x_0 s}{2\pi x_0 s} ds \quad (18)$$

(for a symmetric pattern). The noise amplification is

$$\alpha^2 = \int_{-1}^1 \left[\frac{\psi(s)}{p(s)} \right]^2 ds. \quad (19)$$

If $h(s)$ is any function defined on the interval $(-1, 1)$ that has the properties that $h(0) = h(1) = 0$ and $h(x) > 0$, we can replace $\psi(s)$ with $\psi(s) + \epsilon h(s)$, where ϵ is a small positive quantity. Then, since $\sin(\pi s)/(\pi s) > 0$ for $|s| < \frac{1}{2}$, $d\mu/d\epsilon$ and $d\alpha^2/d\epsilon$ are both > 0 . This shows that the main beam can be narrowed only at the expense of increasing the noise amplification.

There does not seem to be any simple relationship between the sidelobe level and the noise amplification.

When it comes to making a choice for $Q(x,y)$, the desired antenna pattern, it is important to select a function that is not unrealizable with the given antenna pattern. There is a trade-off between resolution and noise amplification; if $Q(x,y)$ is chosen to be too narrow, two results will follow. The first is that the noise amplification will be unacceptably high, regardless of the sidelobe level. The second is that, since the fitting procedure for determining $\Psi(x,y)$ from $Q(x,y)$ and the original pattern $P(x,y)$ makes a compromise between making $\Psi(x,y)$ close to $Q(x,y)$ and amplifying the noise, if $Q(x,y)$ is too narrow (or otherwise ill-suited), the compromise will be to have a large noise-amplification factor and—often—side lobes that oscillate wildly. In other words, what one may get is a pattern that is not a good fit to $Q(x,y)$ because $Q(x)$ has the wrong shape.

e) Discussion

The discussion that has been given here is basically similar to that of Schell (1969), but the problem treated is significantly different; the differences have a considerable influence on the nature of the solution.

The first difference is that we are concerned here with the problem that land-ocean boundaries—with a contrast of the order of 100 K—exist and the accuracy of the measurements of brightness temperature must be considerably better than 1 K. If the effects of the antenna side lobes are not reduced to a very low level, observations over the ocean near land will be useless. Therefore, the goal here is not to improve the spatial resolution in the main lobe, but to reduce the level of the side lobes to a minimum.

A second difference is that the data rate from instruments like SMMR and LAMMR is very high; there is not time enough to Fourier transform the data in real time. At the outset, the limitation was adopted that the estimated brightness temperature must be a linear combination of the antenna temperatures with coefficients that are independent of the antenna temperatures. This leads to the notion of choosing the coefficients so as to produce a certain antenna pattern, rather than to minimize the error in the brightness temperatures.

A third difference is that, while Schell (1969) seems to be interested in cases where the signal-to-noise ratio is high, in our case the signal-to-noise ratio is not so high that significant amplification of the noise can be tolerated. Therefore care has been taken to evaluate the noise amplification factors; some widening of the main beam may be tolerated if it leads to an increase in the signal-to-noise ratio.

f) Pattern matching at higher frequencies

The problem that arises when the same antenna is used to make observations at more than one frequency is that, at the higher frequency, the antenna pattern must be modified so that it matches the pattern at the lowest frequency. Let ν_1 and ν_2 be two frequencies, with $\nu_1 < \nu_2$. First, Ψ_1 —the effective antenna pattern—is found at the lowest frequency. Then, for the higher frequency, it is necessary to find a set of coefficients so that the effective pattern at the higher frequency $\Psi_2 = \Psi_1$, or

$$\psi_2(s) = \psi_1(s) \quad (20)$$

or

$$m_2(s) = \psi_1(s)/p_2(s). \quad (21)$$

The coefficients for the higher frequency are found from the Fourier transform of $m_2(s)$. Since $p_2(s)$ will not be zero anywhere where $\psi_1(s)$ is non-zero, this ratio will not be large anywhere.

V. CONCLUSIONS

The calculations reported in this paper illustrate a method for processing the data from microwave remote-sensing instruments so as to modify the antenna pattern. The main objective in modifying the antenna pattern is to suppress the response in the far sidelobes. The pattern chosen for study is not entirely realistic in that it i) does not have distinct side lobes, and ii) it is azimuthally symmetric. The pattern was chosen so that the values of P_{ij} and R_i could be expressed analytically.

Given a real antenna pattern, these coefficients would have to be calculated by numerical integration. Finding the patterns for various combinations of a^2 , η^2 , and Δx would show how that particular pattern could be modified to advantage. While the details would differ from the results given here, the following general features should still be true:

- 1) It is possible to smooth the antenna temperatures in such a way that the noise is reduced, but only the main lobe is broadened, while the level of the side lobes is reduced.
- 2) Up to a point, it is possible to reduce the level of the side lobes without broadening the main lobe; this can be done with a reasonable loss due to amplification of the receiver noise.

Nature puts a limit on the resolving power of a finite aperture; success in modifying the pattern of a single-dish antenna depends on not asking the impossible. It is not possible to get an estimate of the brightness at a point that is unaffected by the brightness distribution at surrounding points; if we give in to the inevitable and ask for an estimate of the brightness averaged over an area that is not too small, the quality of the results is improved significantly. This can be seen by comparing Figures 1-e and 1-f; the only difference is in the width of the Gaussian used for Q . The price of trying to increase the resolution is a drastically increased level in the side lobes and a huge increase in the noise amplification.

ACKNOWLEDGEMENT

The author thanks Mr. C. Laughlin and Dr. P. Beaudet for many stimulating discussions on this subject.

REFERENCES

- Bracewell, R. (1955): The Fourier Transform and Its Applications, McGraw-Hill Book Co., New York.
- Buck, G.J., and Gustincic, J.J. (1967): IEEE Trans. on Antennas and Propagation, 15, 376.
- Chow, Y.L., and Pelletier, G.A. (1974): Astron. Astrophys. Suppl., 15, 445.
- Classen, J.P., and Fung, A.K. (1974): IEEE Trans. Antennas and Propagation, AP-22, 433.
- Davenport, W.B. Jr., and Root, W.L. (1958): An Introduction to the Theory of Random Signals and Noise, McGraw-Hill Book Co., New York; Chapter 11.
- Emerson, D.T., Klein, U., and Haslam, C.G.T. (1979): Astron. Astrophys., 76, 92.
- Fleming, H.E. (1976): Inversion Methods in Remote Sounding, NASA Publication n-78-12586, p. 325.
- Foster, M. (1961): Journ. S.I.A.M., 9, 387.
- Högbom, J.A. (1974): Astron. Astrophys. Suppl., 15, 417.
- Njoku, E. (1980): Boundary-Layer Meteorology, 18, 79.
- Schell, A.C. (1969): Antenna Theory, ed. Collin & Zucker (Part 2), p. 557-579.
- Stogryn, A. (1978): IEEE Trans. Antennas and Propagation, AP-26, 720.
- Wiener, N. (1960): Extrapolation, Interpolation, and Smoothing of Stationary Time Series, The Technology Press of The Massachusetts Institute of Technology, New York.

TABLE CAPTIONS

Table 1. The noise amplification (α^2) and sidelobe levels for different effective antenna patterns. The widths are given for the -10 db and -20 db sidelobes; the level of the sidelobes are given where there are separate sidelobes. For all of these calculations, $\Delta x = 1$.

Table 2. The same information as Table 1, for $\Delta x = 2$.

Table 3. The full width at half-maximum (FHHM) for each beam and X_{1000} , the distance at which the contribution to the antenna temperature falls off by a factor of 1000. For all calculations, $\Delta x = 1$.

Table 4. The same information as Table 3, but $\Delta x = 2$.

Table 5. Some bandwidth-limited functions and their Fourier transforms.

Table 6. Series expansions of $F_n(x)$.

Table 7. Half-widths for the functions $F_n(x)$.

TABLE 1

 $\Delta x = 1$

<u>a²</u>	<u>S/N</u>	<u>α^2</u>	<u>x = -10 db</u>	<u>x = -20 db</u>	<u>sidelobe level</u>
1.2	10	0.068	3.4	4.7	
1.2	100	0.18	2.7	3.4	21.5
1.2	1000	0.32	2.4	3.2	25.0
1.2	∞	0.56	2.4	3.3	
1.0	10	0.079	3.3	4.4	
1.0	100	0.24	2.6	3.1, 4.1	19.2
1.0	1000	0.50	2.2	2.8	24.3, 24.0
1.0	∞	1.58	2.1	3.1	
0.8	10	0.093	3.2	4.2	
0.8	100	0.32	2.4	2.9, 4.1	17.5, 25.7
0.8	1000	0.97	2.1	2.5, 3.3	18.9, 22.3
0.8	∞	7.86	1.9	2.8	28.7, 29.2
0.5	10	0.12	2.9	3.9	25.7
0.5	100	0.55	2.2	2.6, 4.0	15.4, 22.4
0.5	1000	2.29	1.8	2.1, 3.2, 4.2	14.9, 19.6, 29.3
0.5	∞	235.	1.5	3.0, 4.0	18.2, 19.5, 20.1

TABLE 2

 $\Delta x = 2$

<u>a²</u>	<u>S/N</u>	<u>α^2</u>	<u>x = -10 db</u>	<u>x = -20 db</u>	<u>sidelobe level</u>
1.2	10	0.29	3.4	4.3	26.7
1.2	100	0.71	2.8	3.6, 5.1	17.6, 23.2
1.2	1000	0.99	2.5	3.5, 4.6	19.8, 24.3
1.2	∞	1.05	2.4	3.4	21.1, 25.3
1.0	10	0.34	3.3	4.2	23.6
1.0	100	0.94	2.6	3.5, 5.0	18.3, 24.3
1.0	1000	1.39	2.2	3.1	24.7, 29.4
1.0	∞	1.50	2.1	3.0	
0.8	10	0.41	3.2	4.1	22.2
0.8	100	1.29	2.3	3.3	20.0, 26.3
0.8	1000	2.06	2.0	2.5	20.2, 22.3, 26.5
0.8	∞	2.25	1.9	2.3, 3.2	18.1, 19.9, 24.2
Original Beam			2.4	4.1	
Gaussian a ² = 1			2.1	3.1	

TABLE 3

 $\Delta x = 1$

a^2	S/N	FWHM	\bar{x}_{1000}
1.2	10	3.8	2.9
1.2	100	3.6	2.4
1.2	1000	2.8	2.2
1.2	∞	2.6	1.7
1.0	10	3.7	2.5
1.0	100	3.0	2.7
1.0	1000	2.6	2.1
1.0	∞	2.4	1.5
0.8	10	3.5	2.0
0.8	100	2.9	2.8
0.8	1000	2.5	2.5
0.8	∞	2.2	1.4
0.5	10	3.4	2.2
0.5	100	2.7	2.9
0.5	1000	2.0	3.2
0.5	∞	1.7	3.0

TABLE 4

$\Delta x = 2$

a^2	S/N	FWHM	\times_{1000}
1.2	10	3.4	2.6
1.2	100	2.7	2.9
1.2	1000	2.5	2.2
1.2	∞	2.5	2.2
1.0	10	3.2	2.5
1.0	100	2.5	2.3
1.0	1000	2.3	1.5
1.0	∞	2.3	1.5
0.8	10	3.0	2.6
0.8	100	2.6	2.1
0.8	1000	2.3	2.2
0.8	∞	2.2	2.8
Original Beam		2.4	5.9

Table 5. some bandwidth-limited functions and their Fourier transforms.

Function	Transform	Remarks
$(1 - s^2)^n \Pi(\frac{1}{2}s)$	$2^{n+1} n! \frac{j_n(2\pi x)}{(2\pi x)^n}$	$j_n(x)$ = spherical Bessel function of the first kind.
$(1 - s^2)^{n+\frac{1}{2}} \Pi(\frac{1}{2}s)$	$\sqrt{\pi} 2^{n+1} n! \frac{J_n(2\pi x)}{(2\pi x)^n}$	J_n = Bessel function of the first kind.
$\frac{(-i)^n 2T_n(s) \Pi(\frac{1}{2}s)}{(1 - s^2)^{\frac{1}{2}}}$	$J_n(2\pi x)$	T_n = Chebyshev polynomial of the first kind.
$(-i)^n P_n(s) \Pi(\frac{1}{2}s)$	$x^{-\frac{1}{2}} J_{n+\frac{1}{2}}(2\pi x)$	P_n = Legendre polynomial.
$\cos^n(\frac{1}{2}\pi s) \Pi(\frac{1}{2}s)$	$\frac{2^{1-n} \Gamma(n+1)}{\Gamma(1+\frac{1}{2}n+2x) \Gamma(1+\frac{1}{2}n-2x)}$	

Table 6. Series expansion of $F_n = 2^{n+1} n! j_n(x)/x^n$. The values of a_n are given separately for $n=0$, n even, and n odd. $F_n = a_0 + \sum a_n \cos(n\pi s)$.

	F_1	F_2	F_3
$n = 0$	3/2	11/12	7/10
n even	0	$-10/(n\pi)^2$	$\frac{-2}{(n\pi)^2} - \frac{168}{(n\pi)^4}$
n odd	$\frac{-4}{(n\pi)^2}$	$\frac{6}{(n\pi)^2} - \frac{24}{(n\pi)^4}$	$\frac{-2}{(n\pi)^2} + \frac{120}{(n\pi)^4} - \frac{480}{(n\pi)^6}$
<hr/>			
α_n^2	14/3	198/105	1486/1155

Table 7. Half-widths of the functions $F_n(x) = 2^{n+1} n! \frac{j_n(\pi x)}{(\pi x)^n}$

n	FWHM
0	0.60
1	0.80
2	0.95
3	1.09
4	1.22
5	1.32
6	1.42

FIGURE CAPTIONS

Figure 1. The original antenna pattern and a Gaussian of unit width (Fig 1-a). Computed effective patterns are shown in 1-b to 1-g. The patterns are normalized so that the integral is unity.

Figure 2. The functions $\Psi_n(x)$ for $n = 0, \dots, 5$.

Figure 3. The functions $2^{n+1} n! \frac{j_n(2\pi x)}{(2\pi x)}$, $n = 0, \dots, 4$.

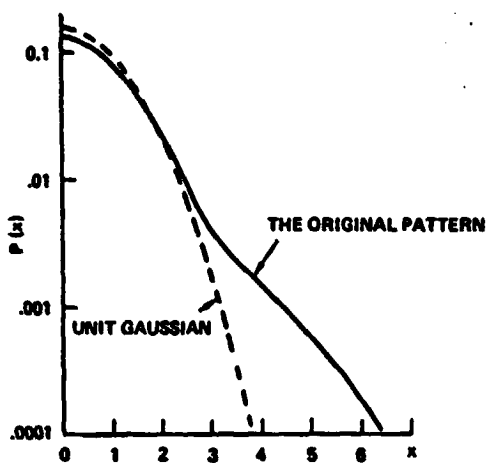


Figure 1-a.

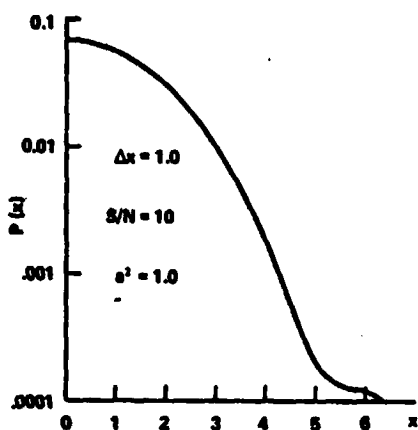


Figure 1-b.

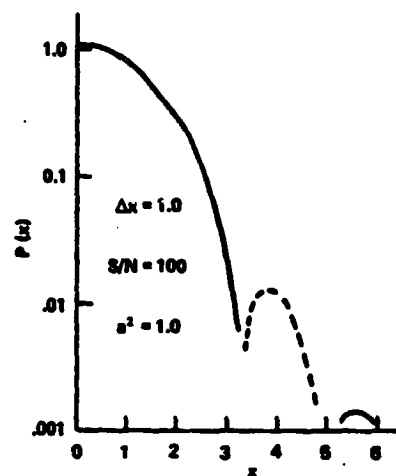


Figure 1-c.

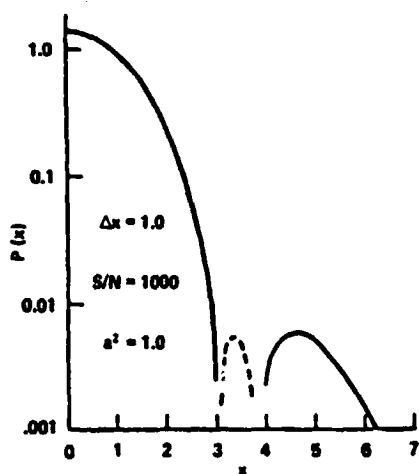


Figure 1-d.

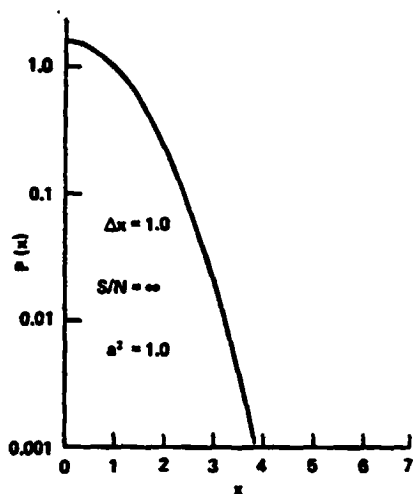


Figure 1-e.

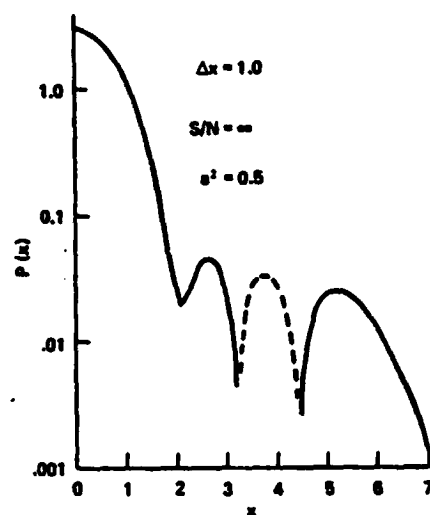


Figure 1-f.

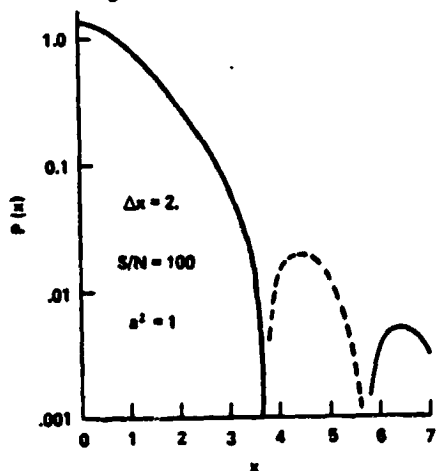


Figure 1-g.

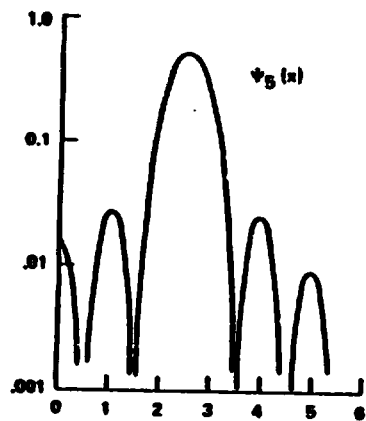
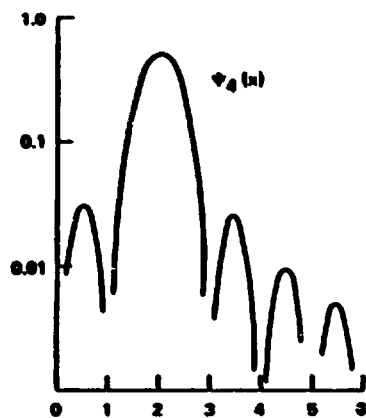
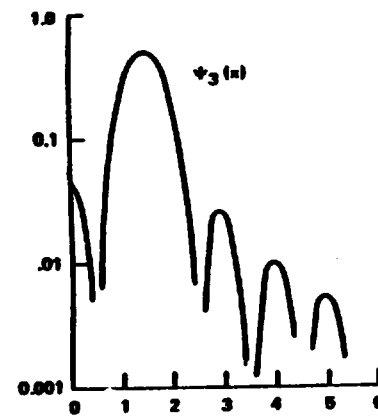
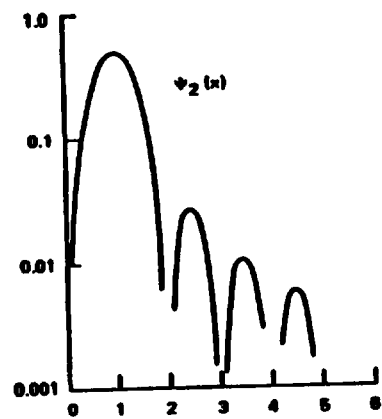
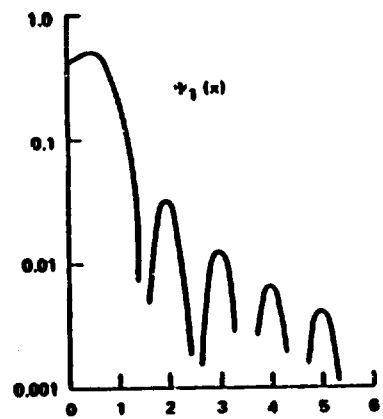
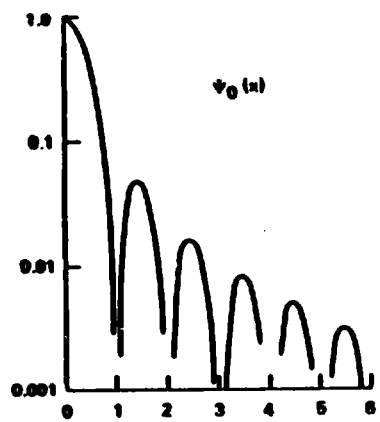


Figure 2.

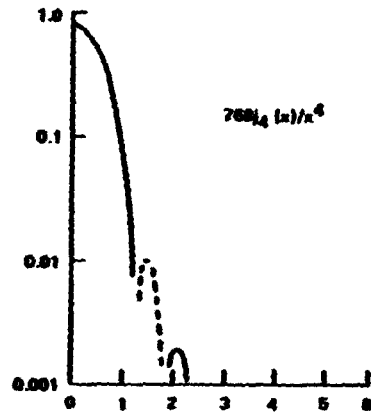
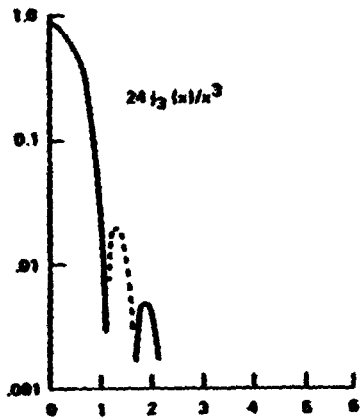
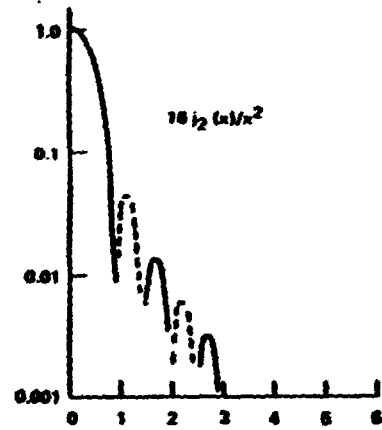
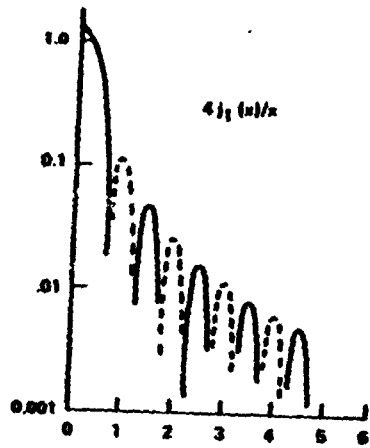
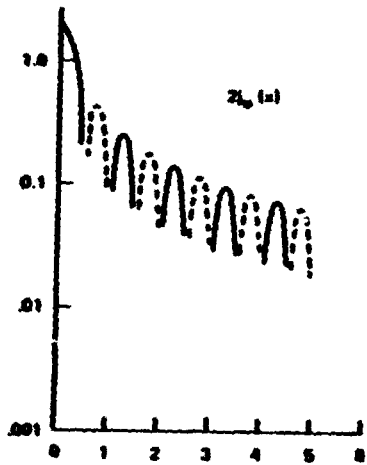


Figure 3.